Simulated and predicted responses of tree stem radial growth to climate change–a case study in semi-arid north central China

Minhui He[a,*], Bao Yang[b], Sergio Rossi[c,d], Achim Bräuning[e], Vladimir Shishov[f], Shuyuan Kang[b]

[a]Center for Ecological Forecasting and Global Change, College of Forestry, Northwest A&F University, 712100 Yangling, China

[b]Key Laboratory of Desert and Desertification, Northwest Institute of Eco-Environment and Resources, Chinese Academy of Sciences, 730000 Lanzhou, China

[c]Département des Sciences Fondamentales, Université du Québec à Chicoutimi, G7H 2B1 Chicoutimi, Canada

[d]Key Laboratory of Vegetation Restoration and Management of Degraded Ecosystems, Guangdong Provincial Key Laboratory of Applied Botany, South China Botanical Garden, Chinese Academy of Sciences, 510650 Guangzhou, China

[e]Institute of Geography, Friedrich-Alexander-University Erlangen-Nürnberg, 91058 Erlangen, Germany

[f]Mathematical Methods and Information Technology Department, Siberian Federal University, 660075 Krasnoyarsk, Russia

[*]Corresponding author: minhuihe@nwafu.edu.cn

Address: Center for Ecological Forecasting and Global Change, College of Forestry, Northwest A&F University, 712100 Yangling, China

Abstract

Precise knowledge how tree growth will respond to future climate change is essential for the adapted management of forest ecosystems. By conducting sensitivity tests, tree-ring process-based cambial growth models can provide an innovative way to better understand wood formation under different climate change scenarios. As a case study in semi-arid north central China, we used artificially increased or decreased daily climatic data as input to the Vaganov-Shashkin dynamic growth model to investigate the response of wood formation to climatic change. By calibrating the tree-ring model using daily climate data over the period 1951–2010, we found that 81% of radial growth was driven by soil moisture, while 13% of growth was controlled by temperature. During the main growing season June–August, significant differences in the integral growth rate occurred after changing precipitation by ± 30% or by decreasing temperature by 3.0 °C ($p < 0.05$). However, increasing temperature showed only modest effects on tree radial growth rate. During the past 60 years, a significant advancement of the starting dates of growth was detected, whereby non-significant variability was found for the ending dates of growth. Contemporaneously, the effect of previous winter temperature (previous December to current January) on cambial growth initiation declined after 1980. Significant differences in the growth onset dates only occurred when temperature was reduced by 4.5 °C or increased by 5.5 °C. Moreover, both the onset and ending dates of growth in the study region were more sensitive to cooling rather than to warming. If temperature will increase by 2°C and precipitation will increase by 30% at the end of this century as predicted by some Earth system models, tree radial growth might increase by 19% in the study region, compared to the average during the period 1952–2010. Consequently, tree stem radial growth is expected to increase under a warming and wetting climatic scenario, but will decrease under drying conditions.

Key words: Process-based model, xylogenesis, tree-ring width series, climate change, sensitivity test, forest ecosystems

1. Introduction

The Earth's climate has changed during the past decades and will continue to change further in the near future (IPCC, 2013). Consequently, terrestrial (Delgado-Baquerizo et al., 2017; Pecl et al., 2017; Peñuelas et al., 2018) and marine (Henson et al., 2017; Hoegh-Guldberg and Bruno, 2012; Sweetman et al., 2017) ecosystems have already clearly and fundamentally responded to such changes. Among these ecosystems, forests are expected to be particularly sensitive, because the long lifespan of trees prevents a prompt adaptation to quick environmental changes (Lindner et al., 2010). Indeed, the relationships between climate and tree growth, hereafter defined as stem radial growth, has been extensively investigated either by traditional dendroclimatology (Dulamsuren et al., 2017; Fan and Bräuning, 2017; Huo et al., 2017; Knutzen et al., 2017; Touchan et al., 2016), or by ecophysiological studies (Allen et al., 2010; Anderegg et al., 2013; Liu et al., 2013). A large part of the studies confirms that water stress caused by drought and/or warming is a main driver of tree mortality and decline in forest productivity (Williams et al., 2013; Zhao and Running, 2010). According to the most recent reports of the Intergovernmental Panel on Climate Change (IPCC), climate will continue to warm. Based on such expectations, simulations of forest ecosystem dynamics require precise knowledge on the future growth of trees under changing climatic conditions.

Reliable climate predictions are crucial for quantifying the impacts of climate change on tree growth. Earth system models are the current state-of-the-art climate models (Bao et al., 2015), which simulate terrestrial and marine ecosystems and offer a common framework for ecological research related to climatic processes, analyses of vulnerability, impacts, and adaptation (Bonan and Doney, 2018). However, these climate change scenarios still exhibit uncertainties and await further improvement (Balaji et al., 2018; Rogers et al., 2017; Stouffer et al., 2017). For example, the model uncertainty for the projected precipitation from five climate models on the Tibetan Plateau represented 60% (Gu et al., 2018). Based on 20 general circulation models from the Coupled Model Intercomparison Project Phase 5 (CMIP5), the magnitude of seasonal and annual precipitation was overestimated in most regions of China (Chen and Frauenfeld, 2014). Hence, in remote areas such as the mountainous regions of north central China, where weather stations are sparse and climatic data are short-term and unevenly distributed, the projections will be more uncertain or unreliable. This holds especially true for precipitation, considering its high spatial variability and its great environmental impacts. As a consequence, predicted changes in precipitation showed relatively large biases appeared in the rainy season from May to September in these areas (Guo et al., 2017; Zhu et al., 2018).

Tree-ring process-based models represent a reliable tool to better understand tree growth under different climate change scenarios. Various process-based models have been developed for tree-ring formation by integrating different related processes (for details, see Guiot et al., 2014). Among the existing models, the Vaganov-Shashkin (VS) model is probably most widely used (Shashkin and Vaganov, 1993; Vaganov et al., 2011). For example, it has been extensively applied in the US and Russia

(Anchukaitis et al., 2006; Arzac et al., 2018; Evans et al., 2006; Popkova et al., 2018), Mediterranean region (Sánchez-Salguero et al., 2017; Touchan et al., 2012) and China (He et al., 2017; Yang et al., 2017; Zhang et al., 2011; Zhang et al., 2016). Specifically, the successful simulations of intra-annual density fluctuations in tree rings confirm that the VS model is suitable to study climate impact on tree-ring structures (Popkova et al., 2018). Different versions or improvements of the VS model have been released. VS-Lite is a simplified descendant of the full VS model and takes monthly, rather than daily, accumulated precipitation and average temperature data as inputs (Tolwinski-Ward et al., 2011). The VS-Oscilloscope is a new visual parameterization approach of the VS model and allowing an easy simulation of tree-ring growth (Shishov et al., 2016).

In this study, we simulated and predicted the response of wood formation to climate change in semi-arid north central China by conducting sensitivity tests from the VS model. We aim to (1) simulate wood formation (including growth rate and xylem phenology) retrospectively for the past sixty years (1951–2010); (2) analyze wood formation on the daily time scale and quantify the respective contributions of precipitation and temperature; and (3) predict the response of wood formation to different climate change scenarios using sensitivity tests. Our analyses tested the following two hypotheses: i) the rate of radial growth is mostly influenced by soil moisture; ii) xylem phenology, i.e. the starting and ending dates of stem growth, is driven by temperature.

2. Material and Methods

2.1 Study site and climate

The study site is represented by an altitudinal transect located between 2400 and 2740 m a.s.l. on the Hasi Mountain (37.0 ºN, 104.5 ºE) in Jingyuan County, Gansu Province, north central China. According to the records of the nearest meteorological station at Jingyuan (36.6 ºN, 104.7 ºE, 1398 m a.s.l.), the mean annual temperature during the period 1951–2010 was 9.1 °C. January was the coldest month with a mean temperature of -7.1 °C and July was the warmest one (22.6 °C on average). Annual precipitation was 231 mm, 81% of which falling during May–September. During the past six decades, we observed significant warming in winter, spring and autumn ($p \leq 0.05$), but not in summer ($p > 0.05$). In particular, June–September temperatures showed a negative trend during 1951–1980, followed by a warming tendency. No trend was observed for seasonal or annual precipitation.

2.2 Tree-ring width chronology

Chinese pine (*Pinus tabulaeformis* Carr.) is the dominant tree species in the study region, mainly dominating the north-facing slopes. A total of 187 increment cores from 110 living trees were extracted at breast height with increment borers. The samples were prepared following standard dendrochronological procedures (Speer

2012) and the established tree-ring width chronology (AD 1698–2010) has been published before (Kang et al., 2012). In this study, we focused on the tree-ring width chronology during the instrumental period 1951–2010.

2.3 VS modelling

The Vaganov-Shashkin (VS) model is based on the assumption that climatic influences are associated nonlinearly with tree-ring growth through controls on the process of cell formation in the developing xylem (Shashkin and Vaganov, 1993; Vaganov et al., 2011). Simulated tree-ring width series are determined by comparing daily temperature and soil moisture budget to growth functions using the most limiting factor (Fritts, 1976). The integral tree-ring growth rate Gr(t) is estimated based on the equation

$$Gr(t) = GrE(t) \times \min \{GrT(t), GrW(t)\},$$

where GrE(t), GrT(t) and GrW(t) are the partial growth rates, calculated independently from solar irradiation, temperature, and soil moisture content, respectively.

Daily precipitation and temperature records from the Jingyuan meteorological station were used as input data. Considering the different elevations between the meteorological station and the tree-ring sampling site, we adjusted the daily temperature by a rate of 0.56 °C/100 m. The most appropriate physiological parameters were determined by iteratively debugging and comparing the difference between the actual and simulated tree-ring width series. To test the performance of the model, the analyzed period was split into a calibration and verification sub-period, and the respective root mean squared error (RMSE) and reduction-of-error statistic (RE) were calculated. We also evaluated the relationships of their first-order difference series between the modeled and actual tree-ring width chronology to show the high-frequency variability. The parameters were calibrated using daily climate data for 1951–1984. The final parameters were applied to generate tree-ring indices for the verification period 1985–2010. The model outputs (GrT, GrW, GrE and Gr) of each year were used for further analyses. Daily integral growth rates were accumulated to estimate annual wood production. We also extracted the starting (start of growing season, SOS) and ending (end of growing season, EOS) dates of growth to study the temporal variability in xylem phenology.

2.4 Sensitivity tests and statistics

We performed sensitivity tests to assess the response of wood formation to different climate change scenarios by progressively modifying the climatic factors introduced into the model. Daily temperature and precipitation were modified by step of 0.5°C and 10%, and within a range of ± 6.5 °C and ± 90%, respectively. Each scenario was conducted independently, resulting in a total of 26 and 18 model simulations under changing temperature and precipitation, respectively. The combined effects of temperature and precipitation were also analyzed by modifying temperature by ± 1–4

°C and precipitation by ± 30%–70%, resulting in 48 simulations. The estimated Gr and xylem phenology dates were extracted from each climatic scenario. We tested for significant mean differences in Gr after changing daily temperature or precipitation using a *t*-test. Data were log-transformed (log x+1) when distribution diverged from normality. Such statistics were also applied to test for the differences in xylem phenology.

The sensitivity of xylem phenology to climatic change was also tested by statistical bootstrap correlations using DendroClim2002 (Biondi and Waikul, 2004). Xylem phenology was the dependent variable and the regressors were the monthly mean temperatures and the monthly sums of precipitation for each year for a time window including the months from previous August to current September. Partial correlations were performed to exclude collinearity within the climate data. Correlations were based on the whole common period 1952–2010, and before and after 1981 to investigate the stationarity of the relationships.

3. Results

By simulating wood formation during the past 60 years, we identified the most sensitive parameters influencing tree growth, represented by minimum soil moisture (W_{min}), the lower range of optimal soil moisture (W_{opt1}), minimum temperature (T_{min}), and the lower range of the optimal temperature (T_{opt1}). Changes of these parameters resulted in substantial differences between the simulated and actual tree-ring width series. Using the estimated parameters (Table 1), we obtained consistent variability during their common period (Fig. 1). The first year (1951) of the meteorological record was excluded to reduce the influence of model initialization. Significant positive correlations between the original as well as their first-order difference series highlight the ability of the process-based VS model in the study region ($p < 0.01$; Table 2). The positive values of the reduction-of-error also indicate robustness of the results. Moreover, even if we changed temperature or precipitation for the sensitivity tests, 81.5% of the correlations (in total 98 correlations) between simulated tree-ring width series and the actual chronology still passed the significance level of $p < 0.05$.

3.1 Wood production and climate

According to the model output, the integral growth rate (Gr) of tree stem radial growth was mostly affected by soil moisture (GrW), temperature (GrT) or solar irradiance (GrE). In particular, GrW limited radial growth from late April (day of year (DOY) 115) to late August (DOY 238) because partial growth rate due to GrW was generally lower than partial growth rate due to GrT (Fig. 2). Temperature mainly influenced Gr from late August to the end of September (DOY 274). On average, soil moisture limited radial growth for 124 days and temperature for 31 days. Consequently, as accumulated from the integral growth rate, 81 and 13% of radial growth was determined by soil moisture and temperature, respectively.

A prominent pattern for the variability of Gr from the sensitivity tests was

revealed (Fig. 3). By separately increasing or reducing precipitation, daily average and maximum growth rates were strongly increased or decreased, respectively, especially during DOY 150–240 (Fig. 3a). However, changes in temperature showed only modest influence on tree radial growth (Fig. 3b). A *t*-test revealed significant differences in Gr during June–August (DOY 150–240) under changing precipitation by ± 30% ($p < 0.05$). Mean Gr became significantly different after a cooling of 3.0 °C ($p < 0.05$). However, increasing temperature showed a modest effect Gr, even under warming by 6.5 °C. A combined effect of changing precipitation and temperature revealed that the growth rate was significantly different between wet and dry conditions (Fig. 3c). Compared to the dry scenarios, a prominent higher growth rate (including mean and maximum Gr) occurred if the climate was wet.

The variability in wood production under different climate change scenarios was further evaluated from the accumulated integral growth rate during the main growing season June–August (Fig. 4). Accordingly, warm and wet condition could definitely enhance wood production (Fig. 4a). Compared to the measured tree-ring width under current climate conditions, the highest variability in wood production could achieve 37.3% with increase of temperature and precipitation by 2 °C and 70%, respectively. Interestingly, wood production reduced under a cooling of 3 °C and increasing precipitation by 30%. Moreover, cooling by 4 °C associated to increasing precipitation (+30%, +50%. +70%) could not stimulate wood production (Fig. 4c). Nevertheless, wood production was consistently reduced under warm and dry or cold and dry situations (Fig. 4b, d), depending on the amplitudes of changing precipitation or temperature. The reduction reached 58% and 62% if precipitation reduced by 70% and temperature changed by ± 4°C.

3.2 Xylem phenology and climate

During the past 60 years, a significant advancement of the starting dates of tree radial growth was found in the study region ($p < 0.05$, Fig. 5a). The initiation dates advanced by 2.3 d/decade. More interestingly, we detected a higher rate of 6.4 d/decade before 1981. However, the rate reduced and was not significant after 1981 ($p > 0.05$). No significant trend of the ending dates of growth from 1952 to 2010 or from 1981 to 2010 was observed (Fig. 5b). However, a prominent advancing tendency occurred before 1981, with a rate of 4.1 d/decade.

The sensitivity of xylem phenology to climate change tested by bootstrap correlations during 1952–2010 showed that SOS was influenced by the temperature of the previous winter (Fig. 6a). Specifically, mean temperature of previous December and current January significantly influenced the onset dates of growth ($p < 0.05$). The effect of monthly precipitation from previous August to current September was not significant (Fig. 6b). Considering EOS, we detected significant influences of summer and early autumn temperature, especially in June, July and September (Fig. 6c). March temperature also positively affected EOS. Precipitation exhibited significant correlations with EOS during previous December (positive), current February (positive) and July (negative) (Fig. 6d). The negative influence in July was probably

caused by the collinearity between temperature and precipitation, because partial correlations further confirmed that the significant correlation with precipitation disappeared when controlled for temperature. Hence, we could not identify a significant correlation between summer precipitation and EOS in the study region. Assembled with different seasonal climatic data, the highest correlation with SOS was found with temperature averaged from previous December to current January ($r = -0.56$, $p < 0.01$), while EOS was mostly determined by June–September temperature ($r = 0.40$, $p < 0.01$) during 1952–2010. More interestingly, the significant correlation between SOS and previous December to current January temperature robustly existed during 1952–1980 (Fig. 6a). However, such correlations disappeared over 1981–2010, under warming conditions. No pattern of such changed correlations for EOS was observed (Fig. 6c, d).

Sensitivity tests indicated significant linear trends for SOS and EOS after changing temperature (Fig. 7, right panel). Significant differences in SOS occurred under a cooling of 4.5 °C or a warming of 5.5 °C ($p < 0.05$). Differences in EOS were not significant even under a warming of 6.5 °C. By independently changing temperature, an average slope of 4–5 d per degree Celsius was revealed for SOS and EOS. In particular, we detected significant differences in the slopes under warming compared the cooling scenario. The slopes of SOS and EOS were -6.1 and 5.4 d per degree Celsius under cooling, reducing to -3.8 and 3.8 d per degree Celsius under warming. In contrast, no clear pattern was observed between xylem phenology and changing precipitation (Fig. 7, left panel). Significant differences in EOS occurred when precipitation was reduced to 60%, whereas increases in precipitation did not influence EOS. Combined effects of changing temperature and precipitation on xylem phenology indicated that warm and wet conditions could advance SOS and delay EOS. On the contrary, cold and dry conditions mainly delayed SOS and advanced EOS. No clear patterns were observed under the warm and dry conditions or cold but wet scenarios for the two xylem phenologies.

4. Discussion

In this study, we analyzed wood formation during the past 60 years (1951–2010) in semi-arid north central China, to evaluate the variability of growth and xylem phenology under different climatic change scenarios. For this purpose, we compared measured and simulated tree growth and then simulated stem radial growth under several climatic scenarios using the process-based Vaganov-Shashkin (VS) model. The high consistency between the actual and simulated tree-ring width series confirms that the VS model is suitable to describe wood formation and to identify climate-growth relationships in the study region. Discrepancies exist in the simulated results which could be due to the fact that actual tree-ring width is not only affected by temperature and precipitation, but also by other climatic or environmental factors that are not integrated in the model. Nevertheless, progressively modifying daily temperature and precipitation in the model represents one alternative way for the simulation of wood formation under different climate change scenarios although

uncertainties should be kept in mind.

Our first hypothesis was confirmed by the results, which revealed that rate of radial growth was mostly influenced by soil moisture. Herein, the soil moisture data were generated by the VS model as a function of daily precipitation, transpiration and runoff (Evans et al., 2006). Since such data may be affected by temperature we recommend some caution when interpreting this aspect. We quantified the respective contributions of temperature (13%) and precipitation induced moisture variability (81%) on tree-ring width series during the past 60 years. In dry regions or areas characterized by shallow soils with limited ability to preserve water, the drought-growth relationships are expected to be strong. Under conditions of low precipitation or limited soil moisture, trees respond with reduced cell growth rates (Chaves et al., 2002; Popkova et al., 2018), smaller cell lumen areas (Belien et al., 2012), or reduced wood production rates (Arend and Fromm, 2007). For example, following an exceptional summer drought in 2015, stems of six species across central Europe sharply ceased radial growth at the onset of the drought event and hardly recovered after the drought event (Dietrich et al., 2019). Drought can substantially reduce gas exchange and induce xylem embolism (Balducci et al., 2015). During the period 1985–2014, the increasing trend of summer drought not only resulted in a reduced wood formation, but also in an acclimation of the hydraulic architecture of *L. sibirica* in Inner Asia (Khansaritoreh et al., 2018). Additionally, tree-ring width chronologies also showed significant correlations with precipitation or drought records during the past six decades in the arid and semi-arid regions of north China (Fang et al., 2010, 2012; Kang et al., 2012; Yang et al., 2014).

The second hypothesis affirming that wood phenology was driven by temperature was also confirmed. The starting and ending dates of growth were influenced by previous winter and current late summer to early autumn temperatures, respectively. Accordingly, warmer climate conditions could induce earlier initiations or later terminations of radial growth. Our simulations support an increasing number of studies illustrating the key role of temperature in determining xylem phenology in cold ecosystems (Deslauriers et al., 2017; Richardson et al., 2018), as well in moist (Lupi et al., 2012; Rossi et al., 2008), as in dry sites (Li et al., 2017). Consistently, experiments conducted in a winter-dormant ecosystem robustly showed that warming treatments directly influence vegetation phenology at both sides of the annual period of vegetation activity (Richardson et al., 2018). A positive correlation was identified between spring phenological phases and March–May temperatures by weekly monitored results during 2008–2016 in Slovenia (Prislan et al., 2019). However, the significant influence of precipitation or drought on the initiation of xylem phenology in some arid study regions (Ren et al., 2017; Ziaco et al., 2018) was not confirmed by our findings. More interestingly, we found that severe drought may trigger an earlier end of growth in our study region. Specifically, in two years (2012 and 2013) of monitored data, a significant influence of drought, but a small effect of temperature on the ending dates was reported for Qilian juniper (*Juniperus przewalskii* Kom.) in cold and arid regions of the northeastern Tibetan Plateau (Zhang et al., 2018). Definitely, their two years monitoring data probably occurred under different weather

conditions and therefore may result in some bias. Notably, input data in our model were only available from the nearest meteorological station located in a valley (1398 m a.s.l.), while the sampling sites were located at higher elevations (2400–2740 m a.s.l.). If soil moisture was not a limiting factor for the onset of growth in the valley, we expect that soil moisture should also not constrain the initiation of growth at higher elevations, considering that precipitation increases with elevation in regions affected by the Eastern Asian monsoons (Lu et al., 2007). In fact, limited monitored data indicate that annual precipitation during 2013 and 2014 at the higher elevation site where our samples were taken was on average 48% higher than at the Jingyuan meteorological station (data not published).

Reliability of the xylem phenological data was based on the significant correlations between the simulated and actual tree-ring width chronology during the past 60 years. Consistent variability was also found with the modeled SOS and EOS in the Qilian Mountains, northwestern China (Zhang et al., 2016). We further compared our simulation with available monitored xylogenesis data in the study region. By using the micro-coring method, Zeng et al. (2018) monitored Chinese pine xylogenesis in the two years 2013 and 2014. Six monitored trees had an average age of 49 ± 10 (mean ± standard deviation) yr and three trees had old ages of 286 ± 16 yr. Cambial activity in 2013 occurred in DOY 111–141 in their two age-classified pines, termination was detected in DOY 207–214. In 2014, the two dates were DOY 142–147 and DOY 218–224, respectively. Considering that our simulation ended in the year 2010, we used daily climate data for the two years 2013 and 2014 and performed the modelling with the estimated parameters in the calibration period. Results showed that the corresponding SOS and EOS were DOY 120–132 and 262–264, respectively. Similar SOS was detected with their monitored data, but with an EOS difference of almost 40 days. The large difference between the monitored (9 trees) and our modelling (110 trees) tree population could explain such results.

During the past 60 years, the advancement of the starting dates of growth was probably induced by the warming trend of winter temperature. The change rate of 2.3 d/decade is in agreement with results conducted on the Tibetan Plateau (2.8 d/ decade) (Yang et al., 2017). In contrast, no pattern was observed for the ending dates of growth because of weak changes of June–September temperature. However, a significant delay of the termination of growth was found on the Tibetan Plateau (Yang et al., 2017). More interestingly, the significant warming over 1981–2010 may have resulted in a reduced effect of previous winter temperatures (previous December to January) on the initiation of growth after 1980. Furthermore, because of the significant cooling trend of June–September temperatures during 1951–1980, termination of the growing season was significantly advanced. However, the ending dates did not show significant delaying trend although significant warming had occurred during 1981–2010. Moreover, as indicated by the sensitivity test, the slopes of starting and ending dates of growth were significantly different under cooling and warming scenarios. We herein propose that xylem phenology in our study region is more sensitive to cooling rather than to warming. Consistent sensitive results were also detected by a three-year reciprocal translocation experiment on the Tibetan

Plateau, which showed that the first flowering date of early spring flowering plants was four times less sensitive to warming than to cooling (Wang et al., 2014). The asymmetric response of plant phenological series to temperature was mostly explained by the plastic and adaptive responses of phenophases to temperature change gradients (Meng et al., 2016). Cambial activity starts when temperature exceeds a critical value (Begum et al., 2013; Li et al., 2013, 2017; Rossi et al., 2008). Monitored results showed that an average value of 4–5 °C of the minimum daily mean temperature is needed for xylogenesis in conifers in Europe and Canada (Rossi et al., 2008). As far as we know, however, there are no available monitored data to confirm this conclusion near our study site. Localized heating and cooling experiments on the stem, as conducted by Gričar et al. (2006, 2007), are needed to provide direct evidence of cambial sensitivity to temperature change in the future.

As predicted by the Earth system models participating in the Coupled Model Intercomparison Project Phase 5 (CMIP5), temperature near the study region will increase by 2°C and precipitation will increase by 30% under the scenario of Representative Concentration Pathway (RCP) 2.6 until the end of this century. Herein, this scenario describes an all-out effort to limit global warming to below 2°C, with emissions decreasing sharply after 2020 until being zero from 2080 onward. Under such climate change scenario, the starting dates of growth would advance by 8.9 days, while the ending dates of growth would delay by 10.4 days, compared to the average during the period 1952–2010. Such warm and wet conditions could definitely benefit forest production, which may increase wood formation at our study site by 19%. Under RCP 8.5 scenario, a business-as-usual scenario with increasing greenhouse gas emissions over time, temperature and precipitation will increase by 4°C and 70%, respectively. Thus, wood formation in our semi-arid study region might increase by up to 34% in the next century. However, such simplified linear relationships between wood formation and climatic data may be misleading since extreme conditions were not considered during our model calibration procedure. Thus, *in situ* experiments and monitoring research are absolutely required in the next step. Since all results presented here were limited by the mechanisms and parameter settings of the model itself, caution should be paid against any over-interpretation. Nevertheless, the presented quantified response of wood production to different climate change scenarios provides a theoretical framework for ecological research related to forest ecosystems, its vulnerability to climate change, and to possible adaptation.

Conclusions

In this study, we simulated and predicted the response of wood formation to climate change by the process-based Vaganov-Shashkin model in semi-arid north central China. Our two hypotheses are confirmed by the results, which revealed that during the period 1952–2010, tree stem radial growth rate was mostly influenced by soil moisture, while xylem phenology (i.e. starting and ending dates of growth) was driven by temperature. The onset of growth significantly advanced, corresponding to a warming trend in winter temperature. In contrast, the linear trend of the ending dates

of growth was not significant. Both the starting and ending dates of growth were more sensitive to climate cooling, compared to the warming scenario. We provide quantitative estimates of wood production variability under different climatic change scenarios that may occur in the future. Our study therefore bears the potential to improve and to test tree growth related forest dynamic models. In a next step, long-term (more than 10 years) monitoring or *in situ* data are expected to validate the modeling results. Similar studies based on other tree ecophysiological models are needed to obtain a consistent picture of forest response to climate change in complex mountain environments.

Acknowledgements

The authors are grateful to the editor and the two anonymous reviewers for their invaluable comments. This study was jointly funded by the National Natural Science Foundation of China (Grants no. 41520104005 and 41325008). It was also supported by the Belmont Forum and JPI-Climate, Collaborative Research Action 'INTEGRATE, An integrated data-model study of interactions between tropical monsoons and extratropical climate variability and extremes' (NSFC grant no. 41661144008). V. Shishov was supported by the Russian Science Foundation (project #14-14-00219 P for simulation approach), the State assignment "Science of Future" (project #5.3508.2017/4.6 for software development). Minhui He appreciates the support by the Alexander von Humboldt Foundation.

Conflict of Interest

The authors declare that the research was conducted in the absence of any commercial or financial relationships that could be construed as a potential conflict of interest.

References

Allen, C.D., Macalady, A.K., Chenchouni, H., Bachelet, D., McDowell, N., Vennetier, M., Kitzberger, T., Rigling, A., Breshears, D.D., Hogg, E.H., Gonzalez, P., Fensham, R., Zhang, Z., Castro, J., Demidova, N., Lim, J.H., Allard, G., Running, S.W., Semerci, A., Cobb, N., 2010. A global overview of drought and heat-induced tree mortality reveals emerging climate change risks for forests. For. Ecol. Manage. 259, 660–684. https://doi.org/10.1016/j.foreco.2009.09.001

Anchukaitis, K.J., Evans, M.N., Kaplan, A., Vaganov, E.A., Hughes, M.K., Grissino-Mayer, H.D., Cane, M.A., 2006. Forward modeling of regional scale tree-ring patterns in the southeastern United States and the recent influence of summer drought. Geophys. Res. Lett. 33, L04705. https://doi.org/10.1029/2005GL025050

Anderegg, W.R.L., Kane, J.M., Anderegg, L.D.L., 2013. Consequences of widespread tree mortality triggered by drought and temperature stress. Nat. Clim. Chang. 3,

30–36. https://doi.org/10.1038/nclimate1635
Arend, M., Fromm, J., 2007. Seasonal change in the drought response of wood cell development in poplar. Tree Physiol. 27, 985–992. https://doi.org/10.1093/treephys/27.7.985
Arzac, A., Babushkina, E.A., Fonti, P., Slobodchikova, V., Sviderskaya, I. V., Vaganov, E.A., 2018. Evidences of wider latewood in *Pinus sylvestris* from a forest-steppe of Southern Siberia. Dendrochronologia 49, 1–8. https://doi.org/10.1016/J.DENDRO.2018.02.007
Balaji, V., Taylor, K.E., Juckes, M., Lautenschlager, M., Blanton, C., Cinquini, L., Denvil, S., Durack, P.J., Elkington, M., Guglielmo, F., Guilyardi, E., Hassell, D., Kharin, S., Kindermann, S., Lawrence, B.N., Nikonov, S., Radhakrishnan, A., Stockhause, M., Weigel, T., Williams, D., 2018. Requirements for a global data infrastructure in support of CMIP6. Geosci. Model Dev. Discuss. 1–28. https://doi.org/10.5194/gmd-2018-52
Balducci, L., Deslauriers, A., Giovannelli, A., Beaulieu, M., Delzon, S., Rossi, S., Rathgeber, C.B.K., 2015. How do drought and warming influence survival and wood traits of *Picea mariana* saplings? J. Exp. Bot. 66, 377–389. https://doi.org/10.1093/jxb/eru431
Bao, J., Feng, J., Wang, Y., 2015. Dynamical downscaling simulation and future projection of precipitation over China. J. Geophys. Res. 120, 8227–8243. https://doi.org/10.1002/2015JD023275
Begum, S., Nakaba, S., Yamagishi, Y., Oribe, Y., Funada, R., 2013. Regulation of cambial activity in relation to environmental conditions: understanding the role of temperature in wood formation of trees. Physiol. Plantarum 147, 46–54. https://doi.org/10.1111/j.1399-3054.2012.01663.x
Belien, E., Rossi, S., Morin, H., Deslauriers, A., 2012. Xylogenesis in black spruce subjected to rain exclusion in the field. Can. J. For. Res. 42, 1306–1315. https://doi.org/10.1139/X2012-095
Biondi, F., Waikul, K., 2004. DENDROCLIM2002: A C++ program for statistical calibration of climate signals in tree-ring chronologies. Comput. Geosci. 30, 303–311. https://doi.org/10.1016/j.cageo.2003.11.004
Bonan, G.B., Doney, S.C., 2018. Climate, ecosystems, and planetary futures: The challenge to predict life in Earth system models. Science 359, eaam8328. https://doi.org/10.1126/science.aam8328
Chaves, M.M., Pereira, J.S., Maroco, J., Rodrigues, M.L., Ricardo, C.P.P., Osório, M.L., Carvalho, I., Faria, T., Pinheiro, C., 2002. How plants cope with water stress in the field? Photosynthesis and growth. Ann. Bot. 89, 907–916. https://doi.org/10.1093/aob/mcf105
Chen, L., Frauenfeld, O.W., 2014. A comprehensive evaluation of precipitation simulations over China based on CMIP5 multimodel ensemble projections. J. Geophys. Res. 119, 5767–5786. https://doi.org/10.1002/2013JD021190
Delgado-baquerizo, M., Eldridge, D.J., Maestre, F.T., Delgado-baquerizo, M., Eldridge, D.J., Maestre, F.T., Karunaratne, S.B., Trivedi, P., Reich, P.B., Singh, B.K., 2017. Climate legacies drive global soil carbon stocks in terrestrial

ecosystems. Sci. Adv. 3, 1–8. https://doi.org/10.1126/sciadv.1602008
Deslauriers, A., Fonti, P., Rossi, S., Rathgeber, C., Gričar, J., 2017. Ecophysiology and plasticity of wood and phloem formation. In: Amoroso M., Daniels L., Baker P., Camarero J. (eds) Dendroecology. Ecological Studies (Analysis and Synthesis), vol 231. Springer, Cham
Dietrich, L., Delzon, S., Hoch, G., Kahmen, A., 2019. No role for xylem embolism or carbohydrate shortage in temperate trees during the severe 2015 drought. J. Ecol. 107, 334–349. https://doi.org/10.1111/1365-2745.13051
Dulamsuren, C., Hauck, M., Kopp, G., Ruff, M., Leuschner, C., 2017. European beech responds to climate change with growth decline at lower, and growth increase at higher elevations in the center of its distribution range (SW Germany). Trees - Struct. Funct. 31, 673–686. https://doi.org/10.1007/s00468-016-1499-x
Evans, M.N., Reichert, B.K., Kaplan, A., Anchukaitis, K.J., Vaganov, E.A., Hughes, M.K., Cane, M.A., 2006. A forward modeling approach to paleoclimatic interpretation of tree-ring data. J. Geophys. Res. Biogeosciences 111, G03008. https://doi.org/10.1029/2006JG000166
Fan, Z.X., Bräuning, A., 2017. Tree-ring evidence for the historical cyclic defoliator outbreaks on *Larix potaninii* in the central Hengduan Mountains, SW China. Ecol. Indic. 74, 160–171. https://doi.org/10.1016/j.ecolind.2016.11.026
Fang, K., Gou, X., Chen, F., D'Arrigo, R., Jinbao, L., 2010. Tree-ring based drought reconstruction for the Guiqing mountain (China): Linkages to the Indian and Pacific Oceans. Int. J. Climatol. 30, 1137–1145. https://doi.org/10.1002/joc.1974
Fang, K., Gou, X., Chen, F., Liu, C., Davi, N., Li, J., Zhao, Z., Li, Y., 2012. Tree-ring based reconstruction of drought variability (1615–2009) in the Kongtong Mountain area, northern China. Glob. Planet. Change 80–81, 190–197. https://doi.org/10.1016/j.gloplacha.2011.10.009
Fritts, H.C., 1976. Tree rings and climate. Academic press, Arizona, USA
Gu, H., Yu, Z., Yang, C., Ju, Q., Yang, T., Zhang, D., 2018. High-resolution ensemble projections and uncertainty assessment of regional climate change over China in CORDEX East Asia. Hydrol. Earth Syst. Sci. 22, 3087–3103. https://doi.org/10.5194/hess-22-3087-2018
Guiot, J., Boucher, E., Gea-Izquierdo, G., 2014. Process models and model-data fusion in dendroecology. Front. Ecol. Evol. 2, 52. https://doi.org/10.3389/fevo.2014.00052
Guo, J., Huang, G., Wang, X., Li, Y., Lin, Q., 2017. Investigating future precipitation changes over China through a high-resolution regional climate model ensemble. Earth's Futur. 5, 285–303. https://doi.org/10.1002/2016EF000433
Gričar, J., Zupančič, M., Čufar, K., Koch, G., Schmitt, U., Primož, P., 2006. Effect of local heating and cooling on cambial activity and cell differentiation in the stem of Norway spruce (*Picea abies*). Ann. Bot. 97, 943–951. https://doi.org/10.1093/aob/mcl050
Gričar, J., Zupančič, M., Čufar, K., Oven, P., 2007. Regular cambial activity and xylem and phloem formation in locally heated and cooled stem portions of Norway spruce. Wood Sci. Technol. 41, 463–475.

https://doi.org/10.1007/s00226-006-0109-2
He, M., Shishov, V., Kaparova, N., Yang, B., Bräuning, A., Grießinger, J., 2017. Process-based modeling of tree-ring formation and its relationships with climate on the Tibetan Plateau. Dendrochronologia 42, 31–41. https://doi.org/10.1016/j.dendro.2017.01.002
Henson, S.A., Beaulieu, C., Ilyina, T., John, J.G., Long, M., Séférian, R., Tjiputra, J., Sarmiento, J.L., 2017. Rapid emergence of climate change in environmental drivers of marine ecosystems. Nat. Commun. 8, 14682. https://doi.org/10.1038/ncomms14682
Hoegh-Guldberg, O., Bruno, J.F., 2012. The impact of climate change on the world's marine ecosystems. Science 328, 1523–1528. https://doi.org/10.1126/science.1189930
Huo, Y., Gou, X., Liu, W., Li, J., Zhang, F., Fang, K., 2017. Climate–growth relationships of Schrenk spruce (*Picea schrenkiana*) along an altitudinal gradient in the western Tianshan mountains, northwest China. Trees - Struct. Funct. 31, 429–439. https://doi.org/10.1007/s00468-017-1524-8
IPCC, 2013. Fifth Assessment Report. Cambridge: Cambridge University Press.
Kang, S., Yang, B., Qin, C., 2012. Recent tree-growth reduction in north central China as a combined result of a weakened monsoon and atmospheric oscillations. Clim. Change 115, 519–536. https://doi.org/10.1007/s10584-012-0440-6
Khansaritoreh, E., Schuldt, B., Dulamsuren, C., 2018. Hydraulic traits and tree-ring width in *Larix sibirica* Ledeb. as affected by summer drought and forest fragmentation in the Mongolian forest steppe. Ann. For. Sci. 75, 30. https://doi.org/10.1007/s13595-018-0701-2
Knutzen, F., Dulamsuren, C., Meier, I.C., Leuschner, C., 2017. Recent climate warming-related growth decline impairs European beech in the center of its distribution range. Ecosystems 20, 1494–1511. https://doi.org/10.1007/s10021-017-0128-x
Li, X., Liang, E., Gričar, J., Prislan, P., Rossi, S., Čufar, K., 2013. Age dependence of xylogenesis and its climatic sensitivity in Smith fir on the south-eastern Tibetan Plateau. Tree Physiol. 33, 48–56. https://doi.org/10.1093/treephys/tps113
Li, X., Liang, E., Gričar, J., Rossi, S., Čufar, K., Ellison, A.M., 2017. Critical minimum temperature limits xylogenesis and maintains treelines on the southeastern Tibetan Plateau. Sci. Bull. 62, 804–812. https://doi.org/10.1016/j.scib.2017.04.025
Lindner, M., Maroschek, M., Netherer, S., Kremer, A., Barbati, A., Garcia-Gonzalo, J., Seidl, R., Delzon, S., Corona, P., Kolström, M., Lexer, M.J., Marchetti, M., 2010. Climate change impacts, adaptive capacity, and vulnerability of European forest ecosystems. For. Ecol. Manage. 259, 698–709. https://doi.org/10.1016/j.foreco.2009.09.023
Liu, H., Park Williams, A., Allen, C.D., Guo, D., Wu, X., Anenkhonov, O.A., Liang, E., Sandanov, D. V., Yin, Y., Qi, Z., Badmaeva, N.K., 2013. Rapid warming accelerates tree growth decline in semi-arid forests of Inner Asia. Glob. Chang. Biol. 19, 2500–2510. https://doi.org/10.1111/gcb.12217

659 Lu, C., Wang, L., Xie, G., Leng, Y., 2007. Altitude effect of precipitation and spatial
660 distribution of Qinghai-Tibetan Plateau. J. Mt. Sci. 25, 655–663.
661 Lupi, C., Morin, H., Deslauriers, A., Rossi, S., 2012. Xylogenesis in black spruce:
662 Does soil temperature matter? Tree Physiol. 32, 74–82.
663 https://doi.org/10.1093/treephys/tpr132
664 Meng, F., Zhou, Y., Wang, S., Duan, J., Zhang, Z., Niu, H., Jiang, L., Cui, S., Li, X.,
665 Luo, C., Zhang, L., Wang, Q., Bao, X., Dorji, T., Li, Y., Du, M., Zhao, X., Zhao,
666 L., Wang, G., Inouye, D.W., 2016. Temperature sensitivity thresholds to
667 warming and cooling in phenophases of alpine plants. Clim. Change. 139, 579–
668 590. https://doi.org/10.1007/s10584-016-1802-2
669 Pecl, G.T., Araújo, M.B., Bell, J.D., Blanchard, J., Bonebrake, T.C., Chen, I.-C.,
670 Clark, T.D., Colwell, R.K., Danielsen, F., Evengård, B., Falconi, L., Ferrier, S.,
671 Frusher, S., Garcia, R.A., Griffis, R.B., Hobday, A.J., Janion-Scheepers, C.,
672 Jarzyna, M.A., Jennings, S., Lenoir, J., Linnetved, H.I., Martin, V.Y.,
673 McCormack, P.C., McDonald, J., Mitchell, N.J., Mustonen, T., Pandolfi, J.M.,
674 Pettorelli, N., Popova, E., Robinson, S.A., Scheffers, B.R., Shaw, J.D., Sorte,
675 C.J.B., Strugnell, J.M., Sunday, J.M., Tuanmu, M.-N., Vergés, A., Villanueva, C.,
676 Wernberg, T., Wapstra, E., Williams, S.E., 2017. Biodiversity redistribution
677 under climate change: Impacts on ecosystems and human well-being. Science
678 355, eaai9214. https://doi.org/10.1126/science.aai9214
679 Peñuelas, J., Sardans, J., Filella, I., Estiarte, M., Llusià, J., Ogaya, R., Carnicer, J.,
680 Bartrons, M., Rivas-Ubach, A., Grau, O., Peguero, G., Margalef, O., Pla-Rabés,
681 S., Stefanescu, C., Asensio, D., Preece, C., Liu, L., Verger, A., Rico, L., Barbeta,
682 A., Achotegui-Castells, A., Gargallo-Garriga, A., Sperlich, D., Farré-Armengol,
683 G., Fernández-Martínez, M., Liu, D., Zhang, C., Urbina, I., Camino, M., Vives,
684 M., Nadal-Sala, D., Sabaté, S., Gracia, C., Terradas, J., 2018. Assessment of the
685 impacts of climate change on Mediterranean terrestrial ecosystems based on data
686 from field experiments and long-term monitored field gradients in Catalonia.
687 Environ. Exp. Bot. 152, 49–59. https://doi.org/10.1016/j.envexpbot.2017.05.012
688 Popkova, M.I., Vaganov, E.A., Shishov, V. V., Babushkina, E.A., Rossi, S., Fonti, M.
689 V., Fonti, P., 2018. Modeled tracheidograms disclose drought influence on *Pinus*
690 *sylvestris* tree-rings structure from Siberian forest-steppe. Front. Plant Sci. 9, 1–
691 12. https://doi.org/10.3389/fpls.2018.01144
692 Prislan, P., Gričar, J., Čufar, K., de Luis, M., Merela, M., Rossi, S., 2019. Growing
693 season and radial growth predicted for *Fagus sylvatica* under climate change.
694 Clim. Change 153, 181–197. https://doi.org/10.1007/s10584-019-02374-0
695 Ren, P., Rossi, S., Camarero, J.J., Ellison, A.M., Liang, E., Peñuelas, J., 2017. Critical
696 temperature and precipitation thresholds for the onset of xylogenesis of
697 *Juniperus przewalskii* in a semi-arid area of the north-eastern Tibetan Plateau.
698 Ann. Bot. 1–8. https://doi.org/10.1093/aob/mcx188
699 Richardson, A.D., Hufkens, K., Milliman, T., Aubrecht, D.M., Furze, M.E.,
700 Seyednasrollah, B., Krassovski, M.B., Latimer, J.M., Nettles, W.R., Heiderman,
701 R.R., Warren, J.M., Hanson, P.J., 2018. Ecosystem warming extends vegetation
702 activity but heightens vulnerability to cold temperatures. Nature 560, 368–371.

https://doi.org/10.1038/s41586-018-0399-1
Rogers, A., Medlyn, B.E., Dukes, J.S., Bonan, G., von Caemmerer, S., Dietze, M.C., Kattge, J., Leakey, A.D.B., Mercado, L.M., Niinemets, Ü., Prentice, I.C., Serbin, S.P., Sitch, S., Way, D.A., Zaehle, S., 2017. A roadmap for improving the representation of photosynthesis in Earth system models. New Phytol. 213, 22–42. https://doi.org/10.1111/nph.14283
Rossi, S., Deslauriers, A., Gričar, J., Seo, J.W., Rathgeber, C.B.K., Anfodillo, T., Morin, H., Levanic, T., Oven, P., Jalkanen, R., 2008. Critical temperatures for xylogenesis in conifers of cold climates. Glob. Ecol. Biogeogr. 17, 696–707. https://doi.org/10.1111/j.1466-8238.2008.00417.x
Sánchez-Salguero, R., Camarero, J.J., Carrer, M., Gutiérrez, E., Alla, A.Q., Andreu-Hayles, L., Hevia, A., Koutavas, A., Martínez-Sancho, E., Nola, P., Papadopoulos, A., Pasho, E., Toromani, E., Carreira, J.A., Linares, J.C., 2017. Climate extremes and predicted warming threaten Mediterranean Holocene firs forests refugia. Proc. Natl. Acad. Sci. 114 (47), E10142–E10150. https://doi.org/10.1073/pnas.1708109114
Shashkin, A., Vaganov, E., 1993. Simulation model of climatically determined variability of conifers' annual increment (on the example of Scots pine in the steppe zone). Russ. J. Ecol. 24, 275–280.
Shishov, V. V., Tychkov, I.I., Popkova, M.I., Ilyin, V.A., Bryukhanova, M. V., Kirdyanov, A. V., 2016. VS-oscilloscope: A new tool to parameterize tree radial growth based on climate conditions. Dendrochronologia 39, 42–50. https://doi.org/10.1016/j.dendro.2015.10.001
Speer JH (2012) Fundamentals of tree ring research. University of Arizona Press, Tucson, USA
Stouffer, R.J., Eyring, V., Meehl, G.A., Bony, S., Senior, C., Stevens, B., Taylor, K.E., 2017. CMIP5 scientific gaps and recommendations for CMIP6. Bull. Am. Meteorol. Soc. 98, 95–105. https://doi.org/10.1175/BAMS-D-15-00013.1
Sweetman, A.K., Thurber, A.R., Smith, C.R., Levin, L.A., Mora, C., Wei, C.-L., Gooday, A.J., Jones, D.O.B., Rex, M., Yasuhara, M., Ingels, J., Ruhl, H.A., Frieder, C.A., Danovaro, R., Würzberg, L., Baco, A., Grupe, B.M., Pasulka, A., Meyer, K.S., Dunlop, K.M., Henry, L.A., Roberts, J.M., 2017. Major impacts of climate change on deep-sea benthic ecosystems. Elem Sci Anth 5, 4. https://doi.org/10.1525/elementa.203
Tolwinski-Ward, S.E., Evans, M.N., Hughes, M.K., Anchukaitis, K.J., 2011. An efficient forward model of the climate controls on interannual variation in tree-ring width. Clim. Dyn. 36, 2419–2439. https://doi.org/10.1007/s00382-010-0945-5
Touchan, R., Shishov, V. V., Meko, D.M., Nouiri, I., Grachev, A., 2012. Process based model sheds light on climate sensitivity of Mediterranean tree-ring width. Biogeosciences 9, 965–972. https://doi.org/10.5194/bg-9-965-2012
Touchan, R., Shishov, V. V., Tychkov, I.I., Sivrikaya, F., Attieh, J., Ketmen, M., Stephan, J., Mitsopoulos, I., Christou, A., Meko, D.M., 2016. Elevation-layered dendroclimatic signal in eastern Mediterranean tree rings. Environ. Res. Lett. 11,

044020. https://doi.org/10.1088/1748-9326/11/4/044020
Vaganov, E.A., Anchukaitis, K.J., Evans, M.N., 2011. How well understood are the processes that create dendroclimatic records? A mechanistic model of the climatic control on conifer tree-ring growth dynamics. Springer, New York 2, 37–75. https://doi.org/10.1007/978-1-4020-5725-0_3
Wang, S.P., Meng, F.D., Duan, J.C., Wang, Y.F., Cui, X.Y., Piao, S.L., Niu, H.S., Xu, G.P., Luo, C.Y., Luo, C.Y., Zhu, X.X., Shen, M.G., Li, Y.N., Du, M.Y., Tang, Y.H., Zhao, X.Q., Ciais, P., Kimball, B., Peñuelas, J., Janssens, I.A., Cui, S.J., Zhao, L., Zhang, F.W., 2014. Asymmetric sensitivity of first flowering date to warming and cooling in alpine plants. Ecology 95, 3387–3398. https://doi.org/10.1890/13-2235.1
Williams, A.P., Allen, C.D., Macalady, A.K., Griffin, D., Woodhouse, C.A., Meko, D.M., Swetnam, T.W., Rauscher, S.A., Seager, R., Grissino-Mayer, H.D., Dean, J.S., Cook, E.R., Gangodagamage, C., Cai, M., Mcdowell, N.G., 2013. Temperature as a potent driver of regional forest drought stress and tree mortality. Nat. Clim. Chang. 3, 292–297. https://doi.org/10.1038/nclimate1693
Yang, B., Kang, S., Ljungqvist, F.C., He, M., Zhao, Y., Qin, C., 2014. Drought variability at the northern fringe of the Asian summer monsoon region over the past millennia. Clim. Dyn. 43, 845–859. https://doi.org/10.1007/s00382-013-1962-y
Yang, B., He, M., Shishov, V., Tychkov, I., Vaganov, E., Rossi, S., Ljungqvist, F.C., Bräuning, A., Grießinger, J., 2017. New perspective on spring vegetation phenology and global climate change based on Tibetan Plateau tree-ring data. Proc. Natl. Acad. Sci. 114, 6966–6971. https://doi.org/10.1073/pnas.1616608114
Zeng, Q., Rossi, S., Yang, B., 2018. Effects of age and size on xylem phenology in two conifers of northwestern China. Front. Plant Sci. 8:2264. https://doi.org/10.3389/fpls.2017.02264
Zhang, J., Gou, X., Zhang, Y., Lu, M., Xu, X., Zhang, F., Liu, W., Gao, L., 2016. Forward modeling analyses of Qilian Juniper (*Sabina przewalskii*) growth in response to climate factors in different regions of the Qilian Mountains, northwestern China. Trees - Struct. Funct. 30, 175–188. https://doi.org/10.1007/s00468-015-1286-0
Zhang, J., Gou, X., Manzanedo, R.D., Zhang, F., Pederson, N., 2018. Cambial phenology and xylogenesis of *Juniperus przewalskii* over a climatic gradient is influenced by both temperature and drought. Agric. For. Meteorol. 260–261, 165–175. https://doi.org/10.1016/j.agrformet.2018.06.011
Zhang, Y., Shao, X., Xu, Y., Wilmking, M., 2011. Process-based modeling analyses of *Sabina przewalskii* growth response to climate factors around the northeastern Qaidam Basin. Chinese Sci. Bull. 56, 1518–1525. https://doi.org/10.1007/s11434-011-4456-5
Zhao, M., Running, S.W., 2010. Drought-induced reduction in global terrestrial net primary production from 2000 through 2009. Science 329, 940–943. https://doi.org/10.1126/science.1192666
Zhu, J., Huang, G., Wang, X., Cheng, G., Wu, Y., 2018. High-resolution projections

of mean and extreme precipitations over China through PRECIS under RCPs. Clim. Dyn. 50, 4037–4060. https://doi.org/10.1007/s00382-017-3860-1

Ziaco, E., Truettner, C., Biondi, F., Bullock, S., 2018. Moisture-driven xylogenesis in *Pinus ponderosa* from a Mojave Desert mountain reveals high phenological plasticity. Plant Cell Environ. 41, 823–836. https://doi.org/10.1111/pce.13152

Table and Figure captions

Table 1 Tree-ring parameters used in this study.

Table 2 Statistical results for the model performance during the two separated calibration (1952–1984) and verification (1985–2010) periods.

Fig.1 Comparison between the actual (black straight line) and simulated (gray dash-dotted line) tree-ring width series during the past 60 years. Both series were standardized for direct comparison.

Fig. 2 Simulated integral growth rate (Gr) and mean relative growth rates due to soil moisture (GrW), temperature (GrT) and solar irradiance (GrE) averaged over the period 1952–2010. Standard deviations are shown as colored bars.

Fig. 3 Variability of integral growth rate (Gr) under different climate change scenarios. Raw data is the Gr under current climate conditions. Note that in (a) and (b) we just showed the limited climate change scenarios for visual comparison.

Fig. 4 Variability of wood production under different climate change scenarios compared to the measured ring width under current climate conditions. Positive and negative values indicate stimulation and inhibition of wood formation, respectively.

Fig. 5 Characteristics of the simulated starting (a) and ending dates (b) of the growing season in the study region. The linear trends as well as the respective statistical results during the three periods 1952–1980 (blue dashed line), 1981–2010 (orange dashed line) and 1952–2010 (black dash-dotted line) are shown.

Fig. 6 Sensitivity of xylem phenology to climatic data tested by statistical bootstrap correlations calculated from previous August to current September for the three periods 1952–2010 (black bars), 1952–1980 (blue bars), and 1981–2010 (red bars). Significant correlations are marked with filled histograms ($p < 0.05$). The months from August to December of the previous yeas are marked with lower case letters on the x-axis.

Fig. 7 Variability of xylem phenology under different climate change scenarios. Olive dots denote the starting dates of growth (SOS), while the red dots indicate the ending dates of growth (EOS). The left and right panels are the scenarios under the change in precipitation and temperature data, respectively. The black triangle is the average xylem phenological data during 1952–2010. Significant linear trends are shown after changed temperature data. "+" means increase, "–" indicates decrease, and 0 denotes no change.

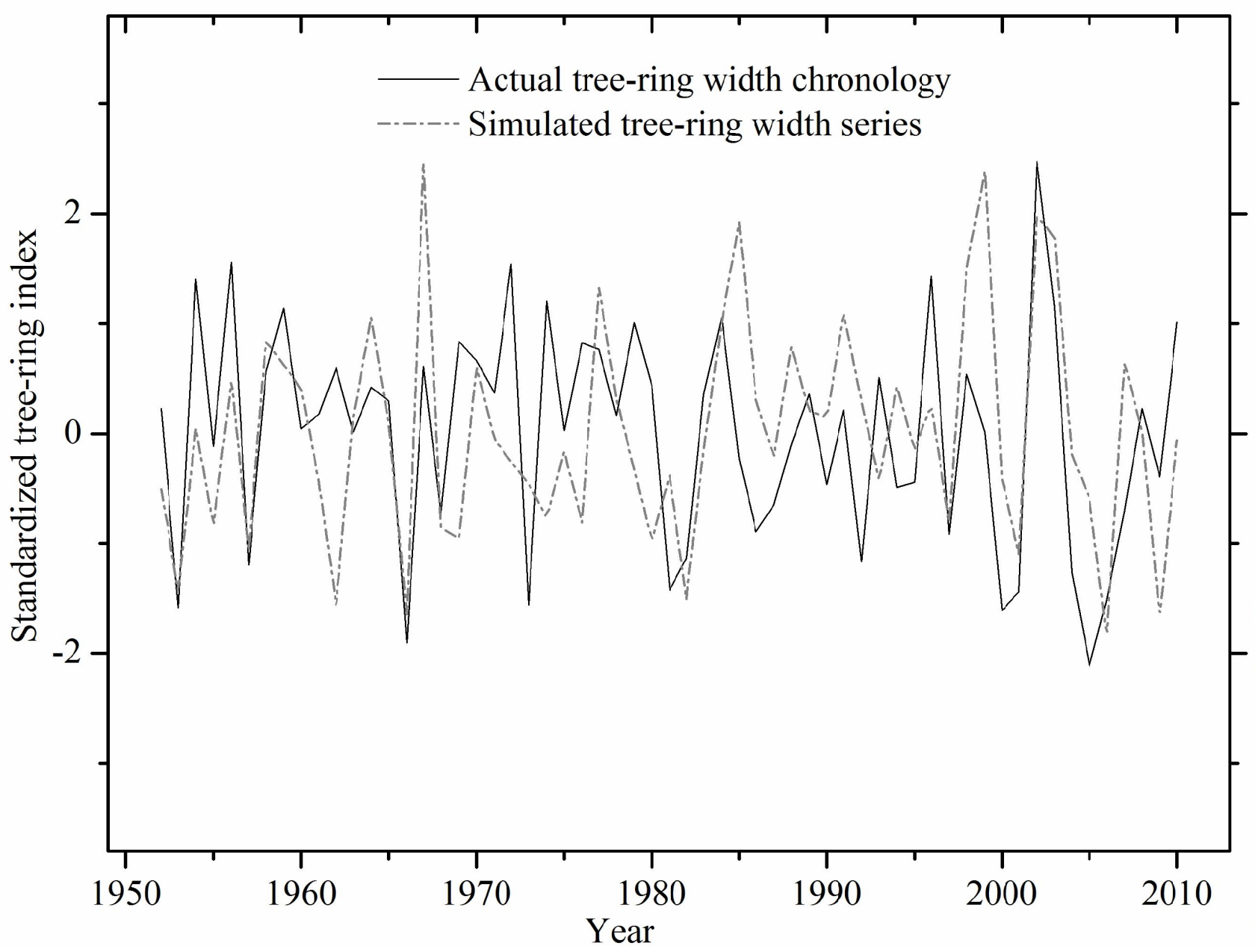
Actual tree-ring width chronology
Simulated tree-ring width series
Standardized tree-ring index
2
0
-2
1950
1960
1970
1980
1990
2000
2010
Year

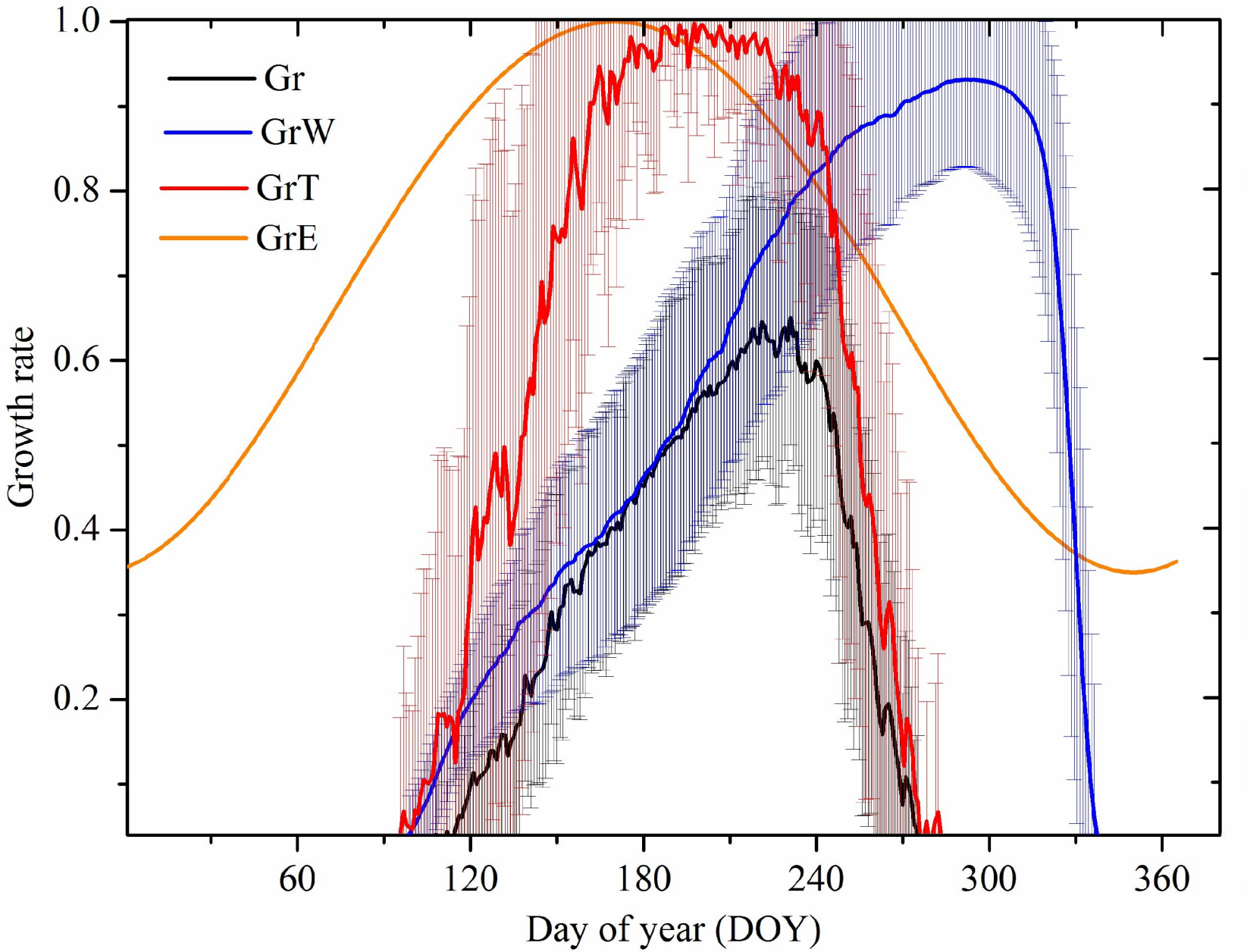
Gr
GrW
GrT
GrE
Growth rate
1.0
0.8
0.6
0.4
0.2
60
120
180
240
300
360
Day of year (DOY)

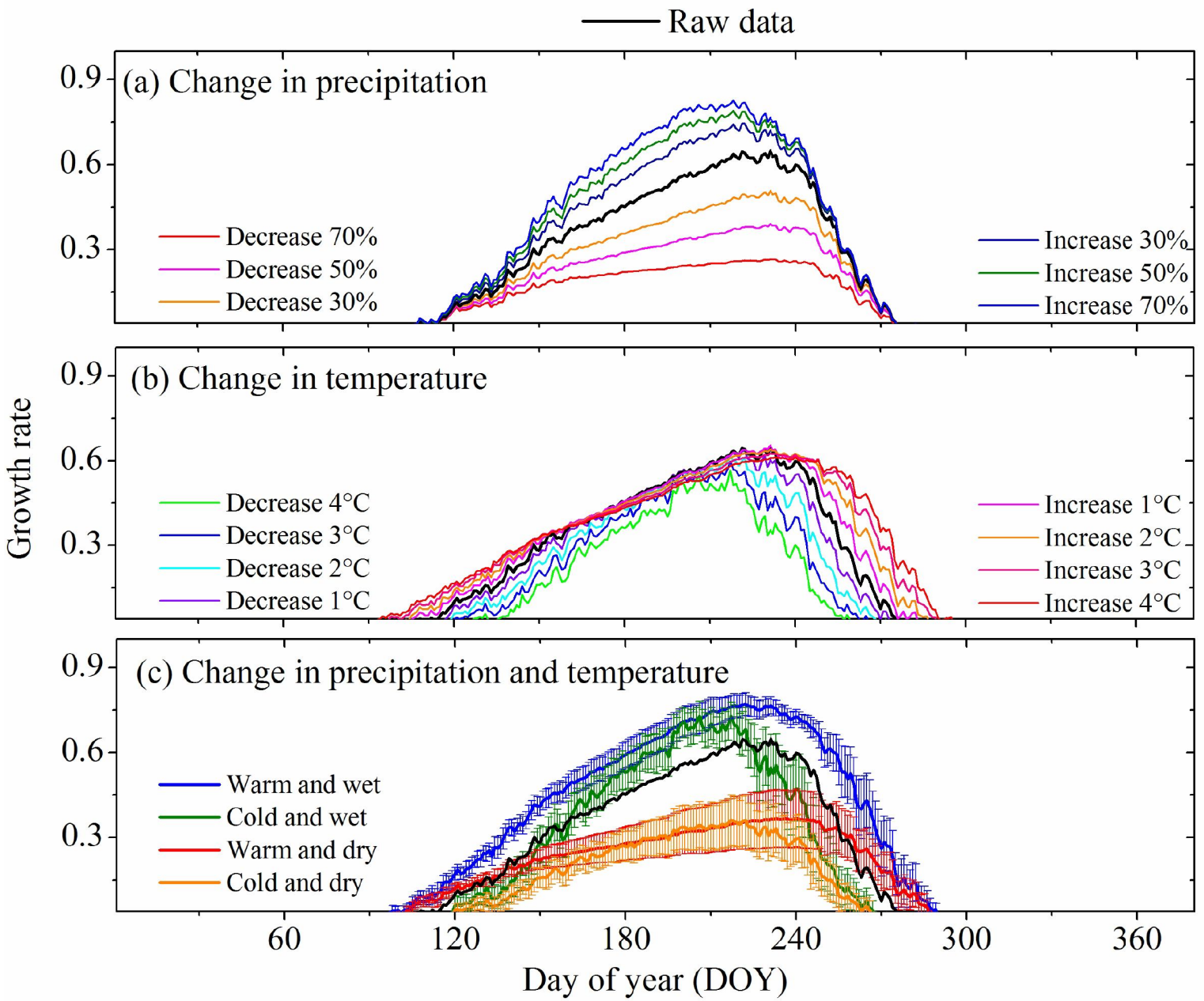
Raw data
(a) Change in precipitation
Decrease 70%
Decrease 50%
Decrease 30%
Increase 30%
Increase 50%
Increase 70%
(b) Change in temperature
Decrease 4°C
Decrease 3°C
Decrease 2°C
Decrease 1°C
Increase 1°C
Increase 2°C
Increase 3°C
Increase 4°C
(c) Change in precipitation and temperature
Warm and wet
Cold and wet
Warm and dry
Cold and dry
Growth rate
0.9
0.6
0.3
60
120
180
240
300
360
Day of year (DOY)

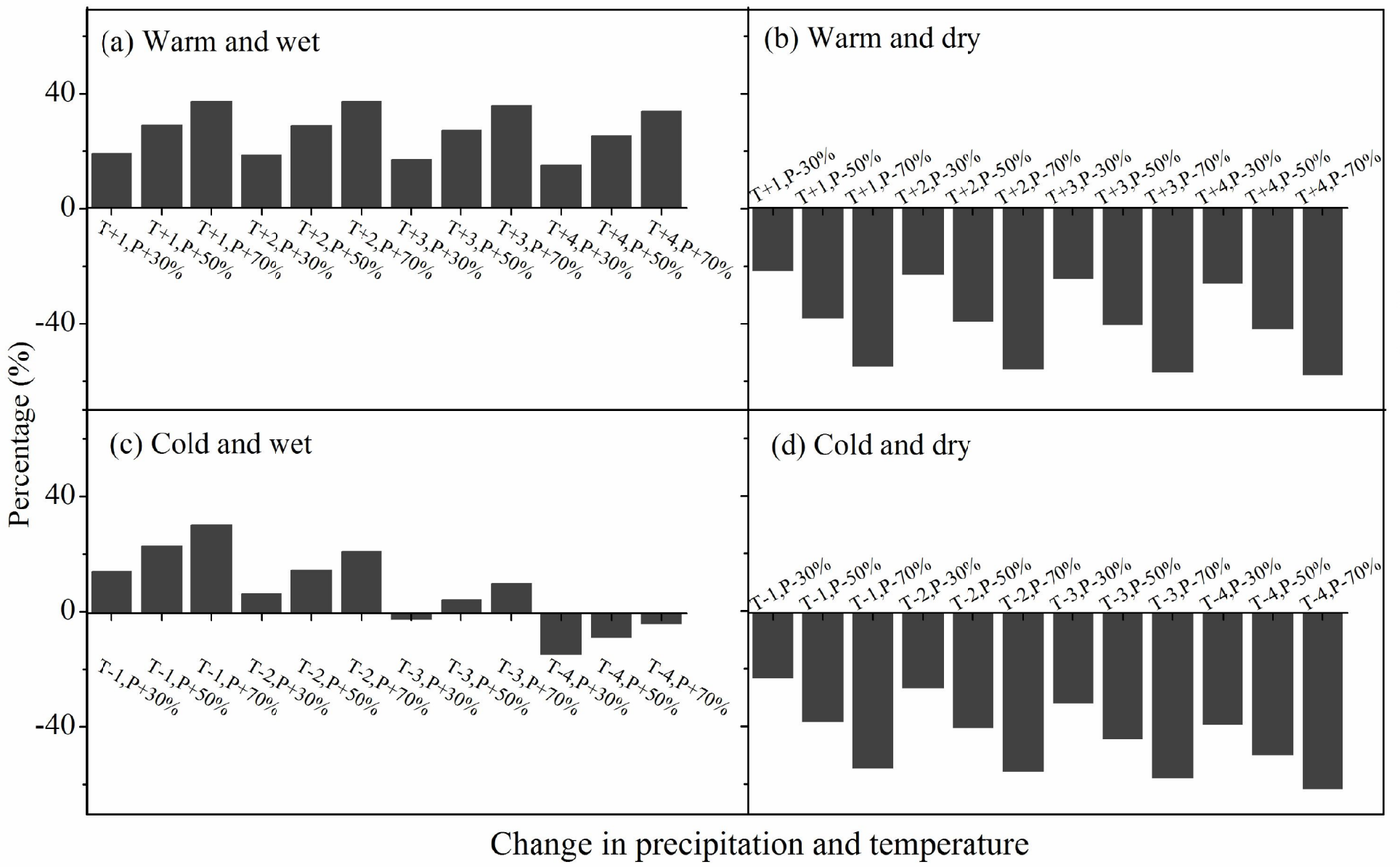
(a) Warm and wet
(b) Warm and dry
(c) Cold and wet
(d) Cold and dry
Percentage (%)
40
0
-40
T+1,P+30%
T+1,P+50%
T+1,P+70%
T+2,P+30%
T+2,P+50%
T+2,P+70%
T+3,P+30%
T+3,P+50%
T+3,P+70%
T+4,P+30%
T+4,P+50%
T+4,P+70%
T+1,P-30%
T+1,P-50%
T+1,P-70%
T+2,P-30%
T+2,P-50%
T+2,P-70%
T+3,P-30%
T+3,P-50%
T+3,P-70%
T+4,P-30%
T+4,P-50%
T+4,P-70%
T-1,P+30%
T-1,P+50%
T-1,P+70%
T-2,P+30%
T-2,P+50%
T-2,P+70%
T-3,P+30%
T-3,P+50%
T-3,P+70%
T-4,P+30%
T-4,P+50%
T-4,P+70%
T-1,P-30%
T-1,P-50%
T-1,P-70%
T-2,P-30%
T-2,P-50%
T-2,P-70%
T-3,P-30%
T-3,P-50%
T-3,P-70%
T-4,P-30%
T-4,P-50%
T-4,P-70%
Change in precipitation and temperature

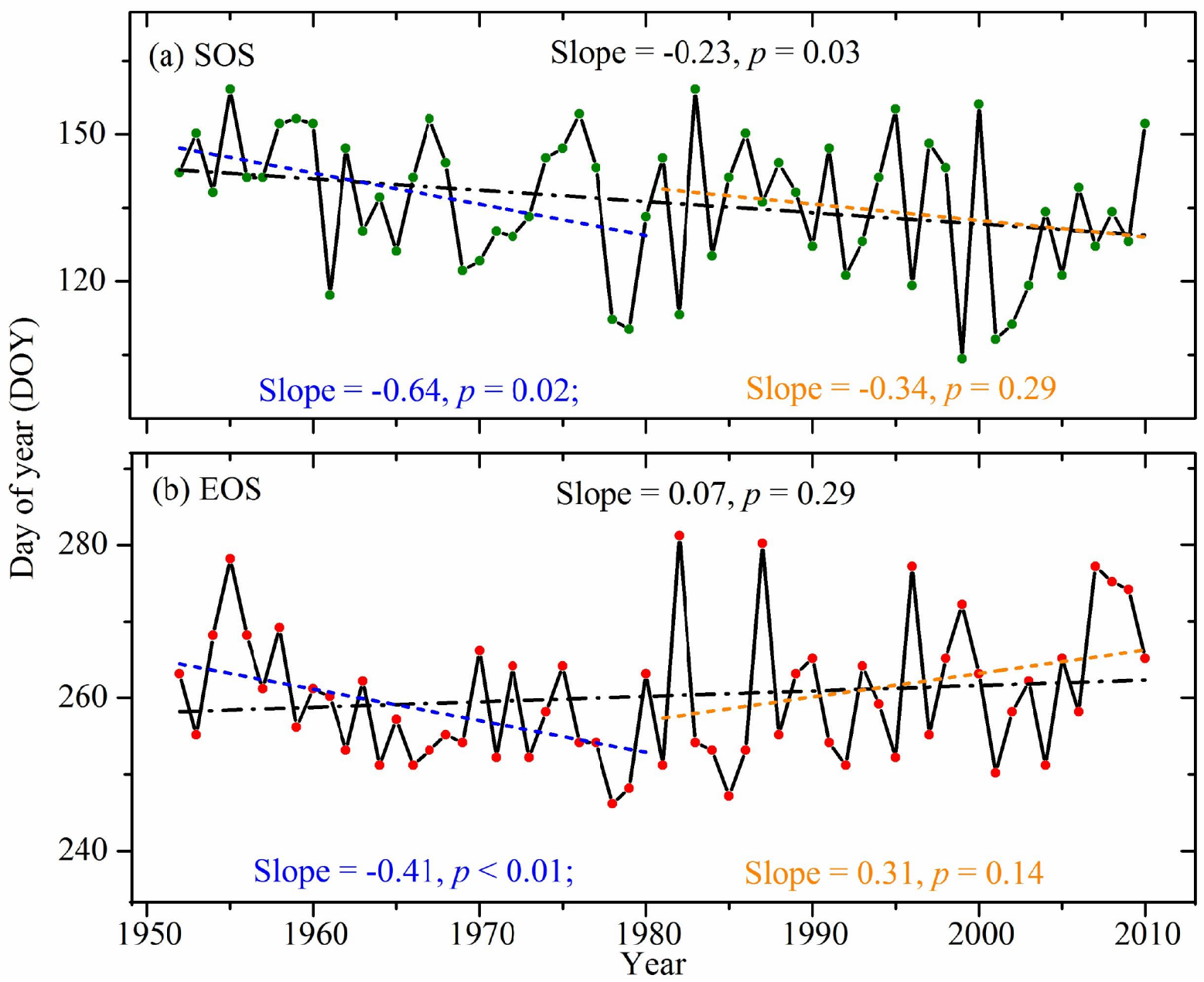
(a) SOS
Slope = -0.23, p = 0.03
Slope = -0.64, p = 0.02;
Slope = -0.34, p = 0.29
(b) EOS
Slope = 0.07, p = 0.29
Slope = -0.41, p < 0.01;
Slope = 0.31, p = 0.14
Day of year (DOY)
Year
150
120
280
260
240
1950
1960
1970
1980
1990
2000
2010

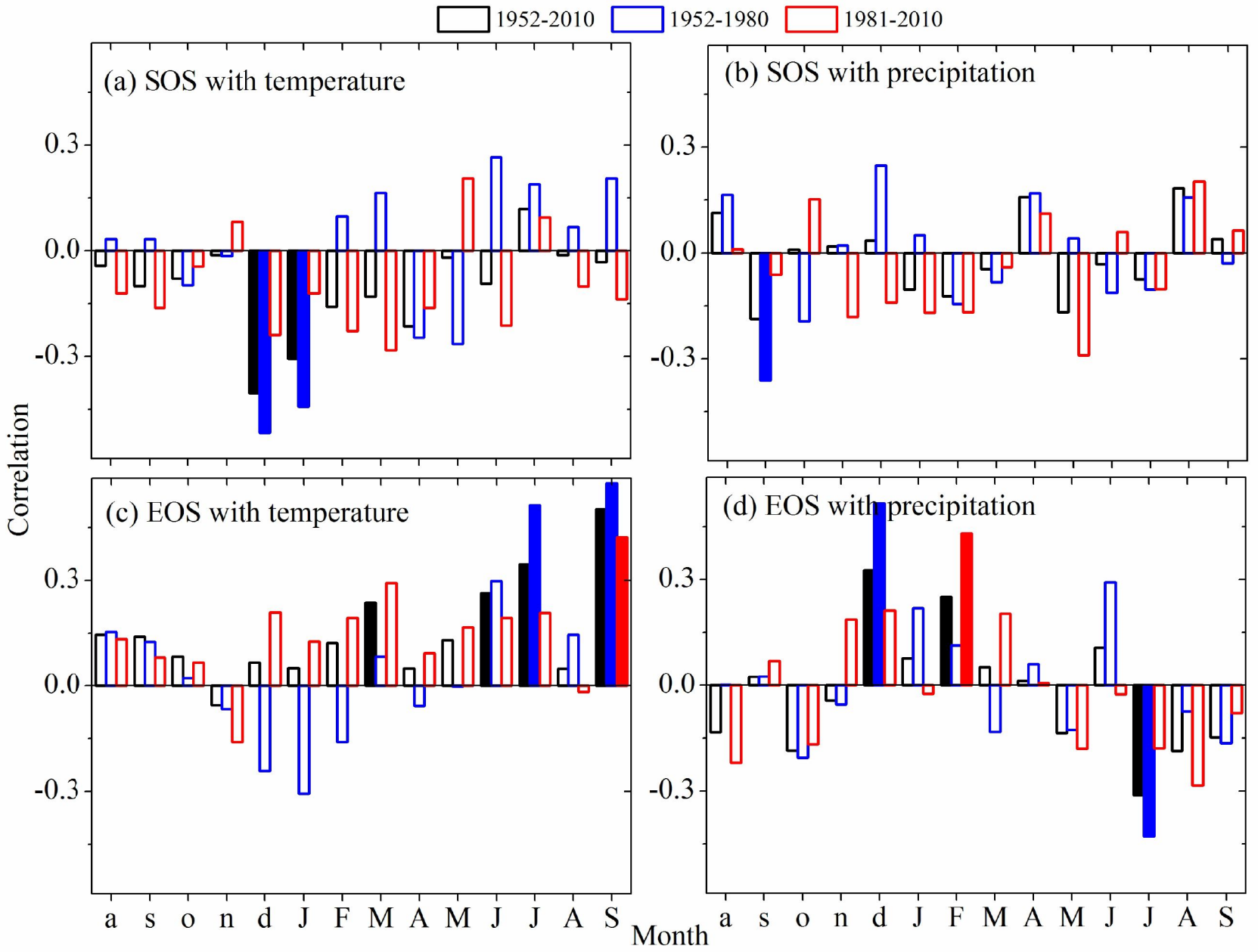
1952-2010
1952-1980
1981-2010
(a) SOS with temperature
(b) SOS with precipitation
(c) EOS with temperature
(d) EOS with precipitation
Correlation
0.3
0.0
-0.3
a s o n d J F M A M J J A S
Month

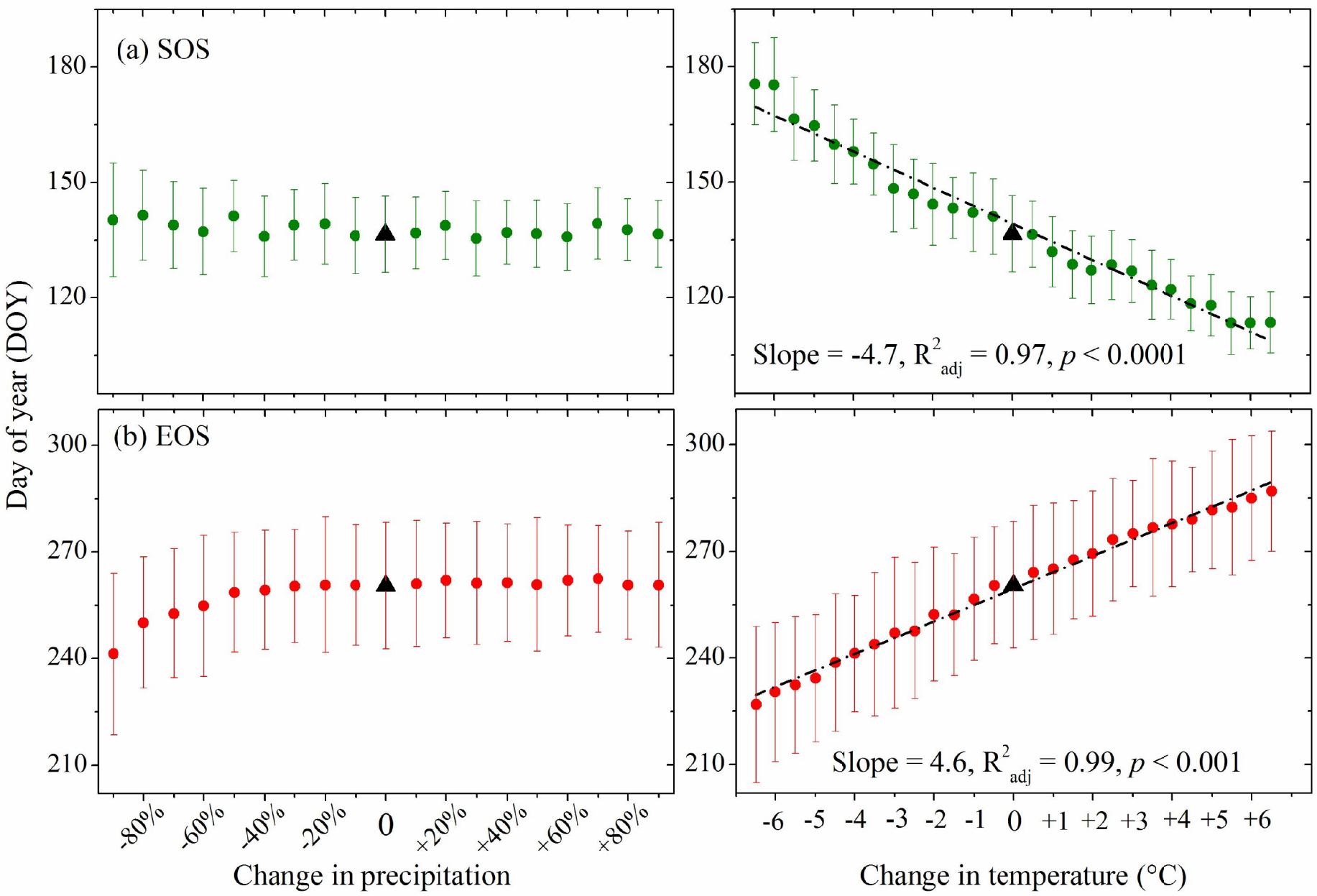
(a) SOS
(b) EOS
Day of year (DOY)
180
150
120
300
270
240
210
Slope = -4.7, R^2_{adj} = 0.97, p < 0.0001
Slope = 4.6, R^2_{adj} = 0.99, p < 0.001
-80% -60% -40% -20% 0 +20% +40% +60% +80%
Change in precipitation
-6 -5 -4 -3 -2 -1 0 +1 +2 +3 +4 +5 +6
Change in temperature (°C)

Table 1 Tree-ring parameters used in this study.

Parameter	Description (Units)	Value
T_{min}	Minimum temperature for tree growth (°C)	7.7
$Topt_1$	Lower end of range of optimal temperatures (°C)	12.5
$Topt_2$	Upper end of range of optimal temperatures (°C)	24.0
T_{max}	Maximum temperature for tree growth (°C)	31.0
W_{min}	Minimum soil moisture for tree growth, relative to saturated soil (v/vs)	0.01
$Wopt_1$	Lower end of range of optimal soil moistures (v/vs)	0.22
$Wopt_2$	Upper end of range of optimal soil moisture (v/vs)	0.31
W_{max}	Maximum soil moisture for tree growth (v/vs)	0.42
W_0	Initial soil moisture (v/vs)	0.08
W_w	Minimum soil moisture (wilting point, v/vs)	0.04
T_{beg}	Sum of temperature to start growth (°C)	40
P_{max}	Maximum daily precipitation for saturated soil (mm/day)	20
K_1	Fraction of precipitation penetrating soil (not caught by crown) (rel. unit)	0.36
K_2	First coefficient for calculation of transpiration (mm/day)	0.06
K_3	Second coefficient for calculation of transpiration (mm/day)	0.12
V_s	Critical growth rate	0.04

Table 2 Statistical results for the model performance during the two separated calibration (1952–1984) and verification (1985–2010) periods.

Period	R	RMSE	RE	R^{-1}	$RMSE^{-1}$
1952–1984	0.48	0.28	0.03	0.50	0.39
1985–2010	0.57	0.29	0.23	0.62	0.33

R: correlation coefficient; RMSE: root mean squared error; RE: reduction-of-error. The superscript -1 indicates that the value is calculated from their first-order difference series.